

REFERENCES

- [1] Konuma, M. *Plasma Techniques for Film Deposition*. India: Alpha Science International, 2005.
- [2] Jamroz, P., and Zyrnicki, W. Optical emission characteristics of glow discharge in the N_2 - H_2 - $Sn(CH_3)_4$ and N_2 - Ar - $Sn(CH_3)_4$ mixtures. *Surface & Coatings Technology*. 201 (2006): 1444 – 1453.
- [3] Qin, S. and McTeer, A. A Nonperturbing Real-Time In Situ Plasma Diagnosis Technique Using an Optical Emission Spectrometer (OES). *IEEE Transactions on Plasma Science*. 34, 4 (August 2006): 1052 – 1058.
- [4] Lebreton, J.-P., Stverak, S., Travnicek, P., etc. The ISL Langmuir probe experiment processing onboard DEMETER: Scientific objectives, description and first results. *Planetary and Space Science*. 54 (2006): 472 – 486.
- [5] Elghazaly, M.H., Abdel baky, A.M., Mansour, M.M., etc. Detailed comparison between probe density measurements of glow discharge in argon and in helium. *Journal of Quantitative Spectroscopy & Radiative Transfer*. 97 (2006): 3963 – 3968.
- [6] Huang, S., Ning, Z.Y., Xin, Y., and Di, X.L. Langmuir probe measurements in inductively coupled CF_4 plasma. *Surface & Coating Technology*. 200 (2006): 3963 – 3968.
- [7] Choi, E.H., Ahn, J.C., Moon, M.W., etc. Electron Temperature and Plasma Density in Surface-Discharged Alternating-Current Plasma Display Panels. *IEEE Transactions on Plasma Science*. 30, 6 (December 2002): 2160 – 2164.
- [8] Corbella, C., Pascual, E., Gomez, M.A., etc. Characterization of diamond-like carbon thin films produced by pulsed-DC low pressure plasma monitored by a Langmuir probe in time-resolved mode. *Diamond & Related Materials*. 14 (2005): 1062 – 1066.
- [9] Friedmann, J.B., Ritter, C., Bisgaard, S., and Shohet, J.L. Automating the analysis of Langmuir probe traces: Construction of an algorithm and sensitivity analysis for probe traces from an electron cyclotron resonance plasma source. *J. Vac. Sci. Technol. A*. 11, 4 (Jul/Aug 1993): 1145 – 1151.

- [10] Park, B.-K., Kim, D.-G., and Kim, G.-H. Analysis of Langmuir Probe Data Using Wavelet Transform. *IEEE Transactions on Plasma Science*. 32, 2 (April 2004): 355 – 361.
- [11] Park, B.-K., and Kim, G.-H. Determination of Plasma Potential from the Langmuir Probe Trace Using Bi-orthogonal Wavelet Transform. *Journal of the Korean Physical Society*. 42 (February 2003): s867 – s872.
- [12] Eliezer, S., and Eliezer, Y. *The Fourth State of Matter*. UK: Institute of Physics, 2001.
- [13] Chapman, B. *Glow Discharge Processes*. The United States: John Wiley & Sons Inc., 1980.
- [14] Shishoo, R. *Plasma Technologies for Textile*. England: Woodhead Publishing, 2007.
- [15] Ngamdee, W. *Measurement of Plasma Parameters with Langmuir Double Probe*. Master's thesis, Graduate School, Chulalongkorn University, 2003.
- [16] Kellman, D.H., Busath, J., and Hong, R. Measurement of Electron Temperature and Density in the DIII-D Neutral Beam Ion Source Arc Chamber. *IEEE Manuscript* (October 12, 1993): 443 – 446.
- [17] Braithwaite, N.St.J., Introduction to gas discharges. *Plasma Source Sci. Technol.* 9 (2000): 517 – 527.
- [18] Mefo, J., Sealy, B.J., Collart, E.J.H., etc. Characterisation of an indirectly heated cathode source using Langmuir probe diagnostics. *NIM B*. 240 (2005): 13 – 17.
- [19] National Instruments. *LabVIEW™ Basics I: Introduction Course Manual*. National Instruments, March 2004.
- [20] OriginLab Data Analysis and Graphing Software. Available from: <http://www.originlab.com/index.aspx?s=8&lm=10> [2007, June 29].
- [21] Paosawatyanong, B. Compensating Langmuir probe studies on the production of high-density plasma in RF transformer coupled discharge. *J. Sci. Res. Chula. Univ.* 29 (2004): 198 – 211.
- [22] Schwabedissen, A., Benck, E.C., and Roberts, J.R. Langmuir probe measurement in an inductively coupled plasma source. *Physical Review*. 55, 3 (March 1997): 3450 – 3458.

- [23] Hopkins, M.B., and Graham, W.G. Langmuir probe technique for plasma parameter measurement in a medium density discharge. *Rev. Sci. Instrum.* 57, 9 (September 1986): 2210 – 2217.
- [24] Chen, F.F. Langmuir Probe Diagnostics. *IEEE-ICOPS meeting*, June 2003.
- [25] UCLA. Available from: <http://www.ee.ucla.edu/~ltptl> [2008, May 10].
- [26] Muakngam, A. *Synthesis Conditions and Raman Spectroscopy Characteristics of the Diamond-like-carbon Thin Films Deposited by RF-PECVD Technique*. Master's thesis, Graduate School, Chulalongkorn University, 2005.
- [27] Ismail, L.Z., and El-Magd, A.A. Pressure Dependence of the Electrical Potential and Electron Temperature in a Microwave-Generated Plasma. *IEEE Transactions on Plasma Science*. 20, 2 (April 1992): 57 – 61.
- [28] Mefo, J., Sealy, B.J., Collart, E.J.H., etc. Langmuir probe analysis of a BF_3 discharge in a high current ion source. *NIM B*. 237 (2005): 245 – 249.

APPENDICES

APPENDIX A

SIMULATION MODEL

To test accuracy of the automated algorithm in analyzing probe data, it is imperative to construct a mathematical model for the probe current as a function of the probe voltage. Based on the I-V characteristic, the model derived from each region, ion-saturation, transition, and electron-saturation regions can be set-up to use as an accuracy test. The probe currents in ion and electron saturation regions should be changed as a function of voltage. The following equations correspond to the linear ion current in the ion-saturation region and the electron-current in the electron-saturation region, respectively [9-11].

$$I_i(V) = m_i V + c_i \quad (\text{A.1})$$

and

$$I_e(V) = m_e V + c_e \quad (\text{A.2})$$

where I and V are the generated data of current and the voltage, m is a slope of straight line whereas c is intercept, and subscriptions of i and e represent the ion and electron, respectively. In the transition region, Maxwellian electron with a single temperature is assumed for data simulation as in the following equation.

$$I_e(V) = I_{e,sat} \exp\left(\frac{V - V_p}{T_e}\right) \quad (\text{A.3})$$

Then, the complete mathematical model for all three voltage intervals is

$$I(V) = \begin{cases} I_i(V) + I_{e,sat} \exp\left(\frac{V - V_p}{T_e}\right), & V \leq V_p \\ I_i(V) + I_{e,sat} + m_e(V - V_p), & V > V_p \end{cases} \quad (\text{A.4})$$

Figure A.1 depicts the generated data that is done by the model.

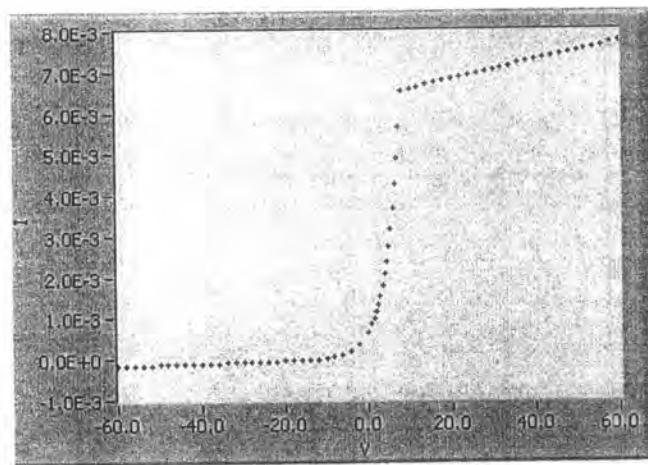


Figure A.1: Showing the simulated I-V characteristic curve.

To make the generated data more realistic, some noises need to be added into the data. The Uniform White Noise Waveform, which is a pattern that Labview already has, is a uniformly distributed pseudorandom pattern whose values are in the range $[-a: a]$, where a is the absolute value of amplitude [19]. In this work, noises with various noise amplitudes are added to the I-V data to evaluate the accuracy of the plasma analysis algorithm. Figure A.2 illustrates the data with several noise levels.

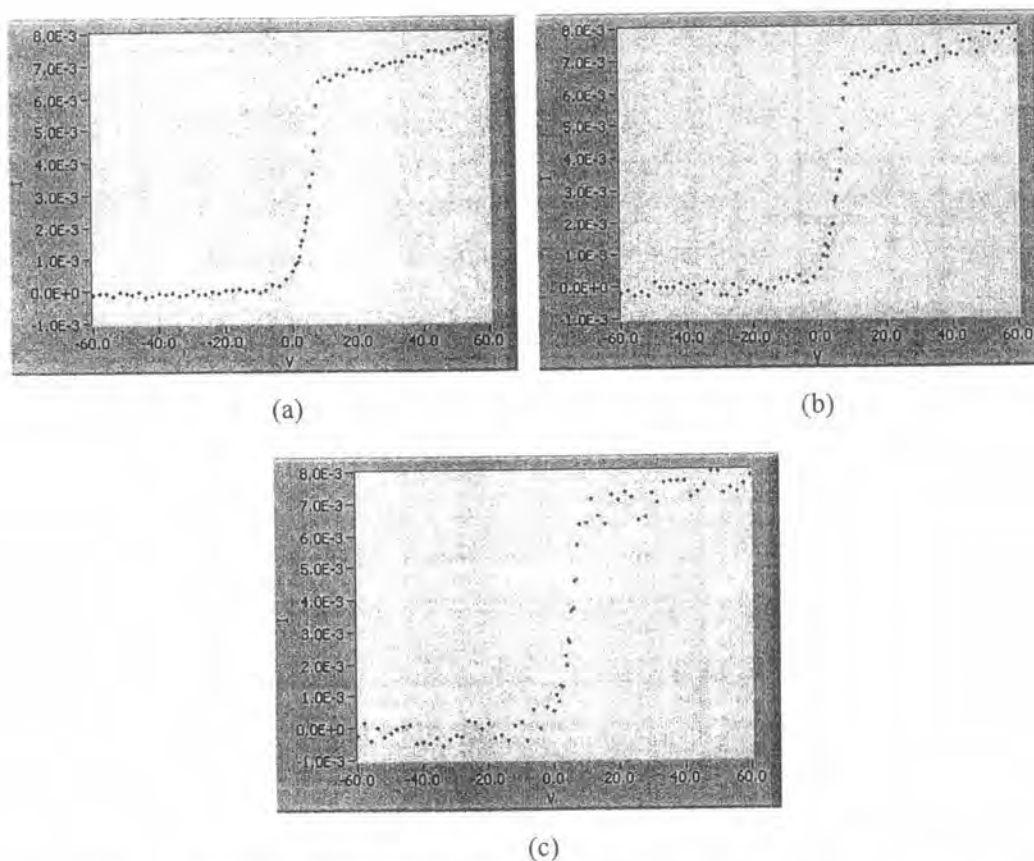


Figure A.2: The generated I-V data with various noise levels of (a) 0.1 mA, (b) 0.3 mA, and (c) 0.5 mA.

To test the automatic algorithm's accuracy, we considered two conditions in the simulation. The first condition concentrated on the accuracy of finding the plasma potential because the input value of the potential in the model defined the intercept of two straight lines in the transition and electron-saturation regions. And the other focus is on the accuracy of the computation of the temperature. In this study, hence, we simulated the I-V data with two conditions to evaluate the accuracy of the algorithm.

As can be seen from figure A.3(a), the automated algorithm can determine plasma potential even when the noise levels increase. But the algorithm still yields the result scattering around the input value (the solid line). It is clearly that the process in separating the three regions by using the characteristics of the first and second derivatives can divide those ranges properly.

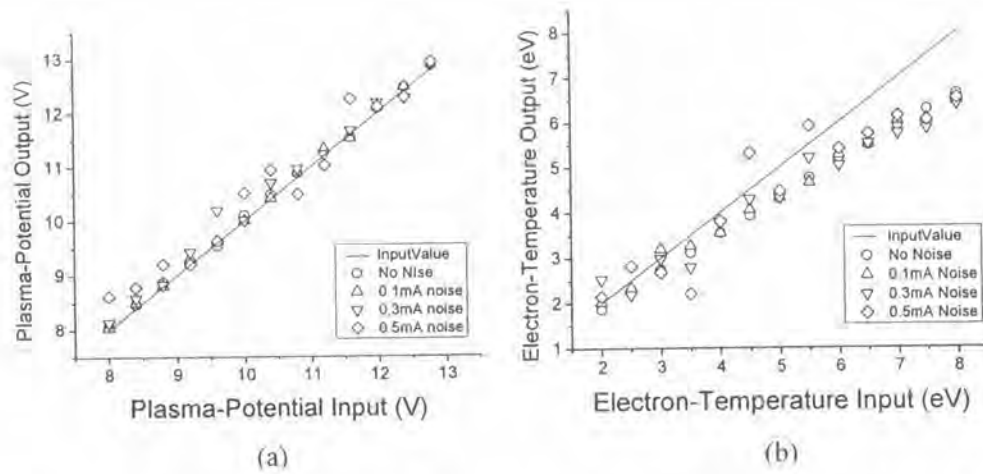


Figure A.3: The analysis result of the simulated data with various noises, (a) plasma potential and (b) electron temperature.

For electron-temperature analysis, the result of the algorithm at high temperatures diverges from the input value (see figure A.3(b)). This is due to the characteristics of the simulated data. The transition-region data couple into the ion-saturation in high temperature range causing data from the transition region falsely taken into consideration as data of the ion-saturation region. This reflects that the simulated data in the ion-saturation region yield inadequate information for saturation current at high temperatures. However, the result only diverts from the input temperature at high temperature. At low temperature, the automated algorithm can perform well in analyzing electron temperature.

APPENDIX B

PROBE ANALYSIS PROGRAM

There is another program that can analyze the single-probe measurement which we could be acquired, Langmuir-probe analyzer (SPA). This program is a commercial program and an automatic analyzer in calculating plasma parameters. The appearance of the SPA analyzer is shown in figure B.1. It is easy to use by importing data of voltage-current and it will return plasma parameters. The result rely on the number of the smoothing points. However, one has to decide the proper smoothing number, since each number may give rather different results.

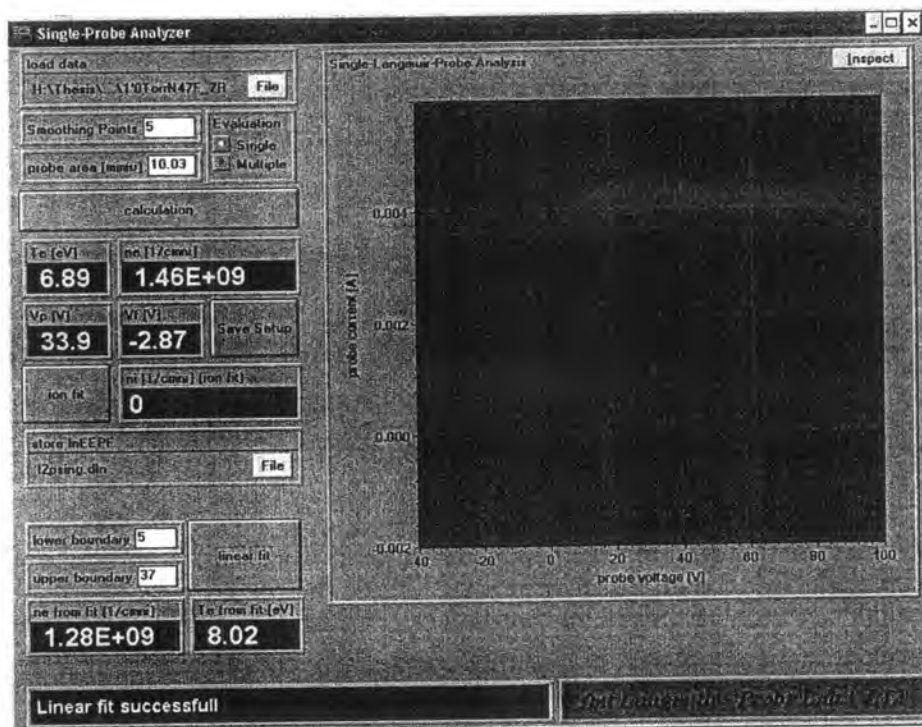


Figure B.1: Appearance of single-Langmuir-probe analyzer (SPA).

In the analytical result of I-V characteristic obtained from RF discharge at dissipated power 20 W, plasma parameters were analyzed with the manual calculation, the automated algorithm, and SPA program as shown in figure B.2. Floating potential tends to decrease when pressure increase. SPA program yields floating potential between -2 and -7 V with ± 0 V in figure B.2a. For plasma potential, SPA program yields the potential lesser than the manual calculation and the automated algorithm in figure B.2b. The difference of plasma potential may come from the defining of potential. SPA program may define plasma potential at the maximum of the first derivative. This maximum generally yields plasma potential lesser than the intercept of two linear fitting in transition and electron-saturation region.

For electron temperature, SPA program can only estimate high electron temperature as the automated algorithm does. In this case, we shall only show the result of high temperature in figure B.2c. SPA program yields the temperature around 7 – 8 eV with ± 1.1 eV at pressure from 0.5 to 1.0 torr. But, only at pressure 1.1 torr, SPA program yields 3.13 ± 1.1 eV which is lower than the manual calculation and the automated algorithm. For electron density at pressure between 0.5 and 0.8 torr in figure B.2d, SPA program and the automated algorithm well agree with the manual calculation. But at high pressure, electron density of SPA program is lower than the manual calculation and the automated algorithm. The density of SPA program decreases from $(2.50 \pm 0.88) \times 10^9 \text{ cm}^{-3}$ to $(3.44 \pm 0.88) \times 10^8 \text{ cm}^{-3}$ with increasing pressure.

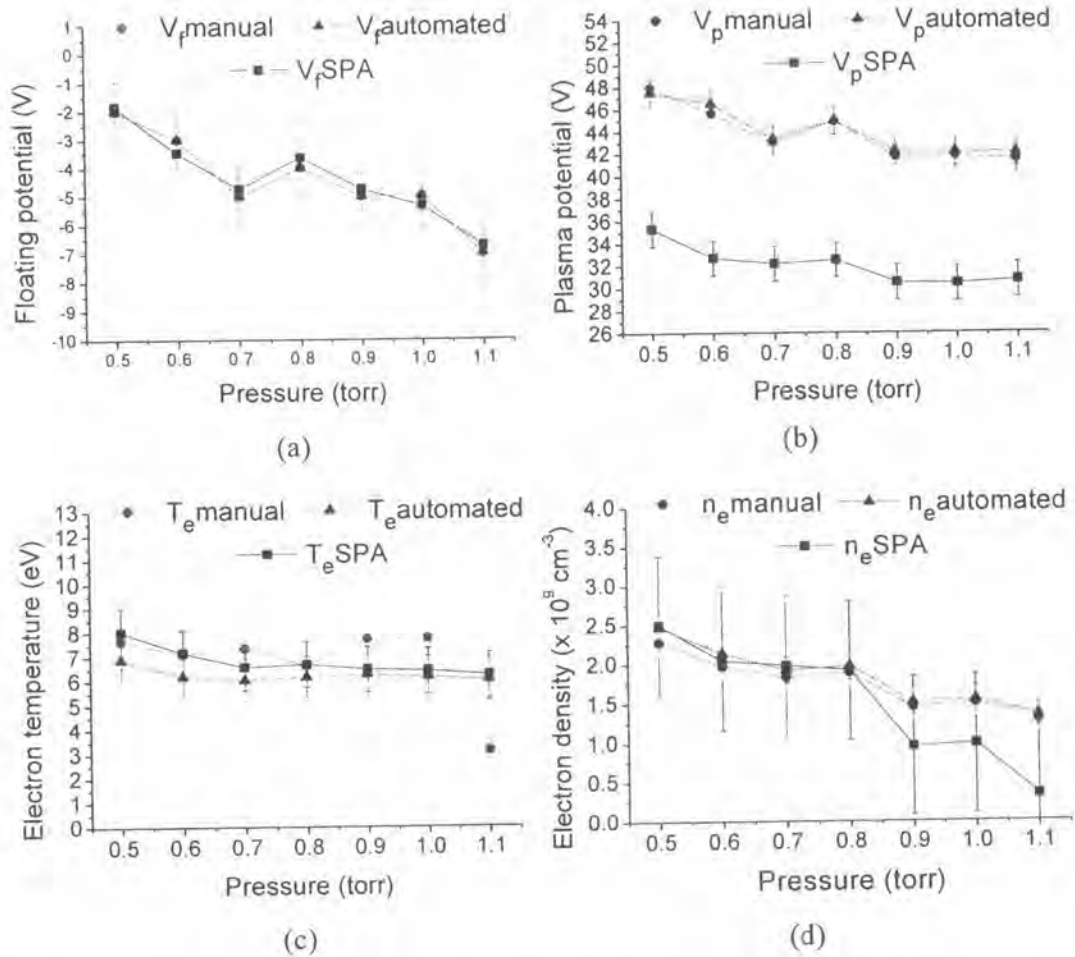


Figure B.2: The analytical result of plasma parameters (a) floating potential, (b) plasma potential, (c) electron temperature, and (d) electron density between the manual calculation and the automated algorithm.

BIOGRAPHY

NAME Mr.SURAKARN THITIANAN
BIRTH 14 NOVEMBER 1981
EDUCATION 2000 – 2003 Bachelor's Degree, Department of Physics, Faculty of Science, Chulalongkorn University.

PUBLICATION

- S. Thititanan, M. Tienprateep, B. Paosawatyanong. Automated Plasma Parameter Measuring System Using Electrical Probes. *Proceeding of the Siam Physics Congress*, Khao Yai, Nakhon Ratchasima (March 20-22, 2008)
- S. Thititanan, M. Tienprateep, B. Paosawatyanong. The Development of Automated Plasma Parameters Analytic Algorithm for Electrical Probe Measurement. *Proceeding of the 13th International Annual Computational Science and Engineering*, Kasetsart University, Bangkok (March 25-27, 2009)

